ChemPubSoc Europe

DOI: 10.1002/chem.201602467

CHEMISTRY
A European Journal
Full Paper

Homogeneous Catalysis

α-Diamine Nickel Catalysts with Nonplanar Chelate Rings for Ethylene Polymerization

Heng Liao,[a, b] Liu Zhong,[b] Zefan Xiao,[b] Ting Zheng,[b] Haiyang Gao,*[a] and Qing Wu[a]

Abstract: A series of novel α-diamine nickel complexes, (ArNH-C(Me)-(Me)C-NHAr)$NiBr_2$, **1:** Ar = 2,6-diisopropylphenyl, **2**: Ar = 2,6-dimethylphenyl, **3**: Ar = phenyl), have been synthesized and characterized. X-ray crystallographic analysis showed that the coordination geometry of the α-diamine nickel complexes is markedly different from conventional α-diimine nickel complexes, and that the chelate ring (N-C-C-N-Ni) of the α-diamine nickel complex is significantly distorted. The α-diamine nickel catalysts also display different steric effects on ethylene polymerization in comparison to the α-diimine nickel catalyst. Increasing the steric hindrance of the α-diamine ligand by substitution of the *o*-methyl groups with *o*-isopropyl groups leads to decreased polymerization activity and molecular weight; however, catalyst thermal stability is significantly enhanced. Living polymerizations of ethylene can be successfully achieved using **1**/Et_2AlCl at 35 °C or **2**/Et_2AlCl at 0 °C. The bulky α-diamine nickel catalyst **1** with isopropyl substituents can additionally be used to control the branching topology of the obtained polyethylene at the same level of branching density by tuning the reaction temperature and ethylene pressure.

Introduction

Late transition-metal catalysts have received much attention since Brookhart and co-workers discovered bulky α-diimine nickel and palladium catalysts for olefin polymerization.[1] A key feature for producing high-molecular-weight polymers lies in suppression of chain transfer by the steric bulk of the *o*-aryl substituents (Figure 1 A). The *o*-aryl substituents are located in an axial position above and below the coordination plane; as a consequence of the perpendicular arrangement of the aryl rings with respect to the coordination plane, this can significantly slow down chain-transfer reactions by associative displacement or chain transfer to bound monomer.[2] On the basis of blocking the axial sites above and below the chelate plane, late transition-metal catalysts with 5- or 6-membered planar chelate rings have been extensively developed, such as α-diimine,[1–3] β-diketiminato,[4] anilido–imino,[5] salicylaldimino,[6] and bis(imino)pyridine ligands.[7] Numerous studies have also established that the aryl substituents closely effect the steric environment of the nickel metal, thus greatly influencing polymerization reactivity and polymeric microstructure.[8] Despite these contributions, none of the aforementioned studies have elucidated how the steric effect operates for ethylene polymerization if the chelate ring is nonplanar and largely distorted.

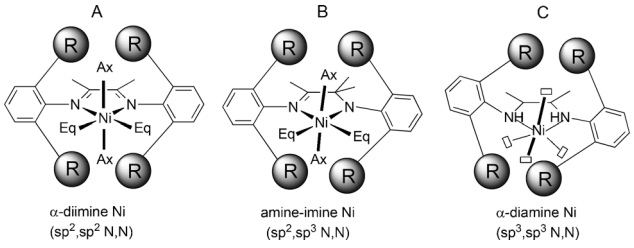

Figure 1. Coordination geometries of nickel catalysts bearing α-diimine, amine-imine, and α-diamine ligands.

Indeed, planar chelating rings are usually formed by conjugating effects, and few nickel catalysts with largely distorted chelate rings for olefin polymerization have been reported to date.[1–6] Our previous investigations have addressed the role that the N–Ni combination plays in the coordination geometry of nickel and polymerization reactivity.[9] α-Diimine nickel catalysts with two sp^2 hybrid nitrogen donor atoms confer a coordination plane which is nonliving systems for ethylene polymerization.[2d,3a] However, hemilabile amine–imine nickel catalysts with sp^3 and sp^2 hybrid nitrogen donor atoms adopt a slightly distorted planar chelating ring system (Figure 1 B), which can polymerize ethylene in a living fashion at elevated temperatures.[9a–d] This highlights the powerful influence of the steric environment around the nickel metal originating from alternation of N–Ni combination on ethylene polymerization reactivity. We can envision that an α-diamine nickel catalyst chelating two sp^3 hybrid nitrogen donor atoms with tetrahedral configuration possesses a largely distorted chelate ring (Fig-

[a] Dr. H. Liao, Prof. H. Gao, Prof. Q. Wu
School of Materials Science and Engineering, PCFM Laboratory
Sun Yat-sen University, Guangzhou 510275 (China)
E-mail: gaohy@mail.sysu.edu.cn

[b] Dr. H. Liao, Dr. L. Zhong, Dr. Z. Xiao, Dr. T. Zheng
School of Chemistry and Chemical Engineering, GD HPPC Laboratory
Sun Yat-sen University, Guangzhou 510275 (China)

Supporting information for this article can be found under http://dx.doi.org/10.1002/chem.201602467.

ure 1 C), which can be used as a nickel catalyst model to study the influences of chelate ring geometry and the N–Ni combination on ethylene polymerization. Herein, we report the successful synthesis of novel α-diamine nickel complexes with five-membered nonplanar chelate rings and their living characteristics for ethylene polymerization. We also demonstrate that the steric bulk of the *o*-aryl substituent of the α-diamine ligand has a critical influence on the coordination and insertion of ethylene, chain transfer, and chain walking, thereby greatly influencing the microstructure of the resulted polymer.

Results and Discussion

The α-diamine ligands (ArNH–C(Me)–(Me)C–NHAr, **L1:** Ar = 2,6-diisopropylphenyl, **L2**: Ar = 2,6-dimethylphenyl, **L3**: Ar = phenyl) containing various *o*-aryl substituents were readily prepared in high yield by a reduction reaction of the corresponding α-diimine compound with excessive $LiAlH_4$ (Scheme 1). All

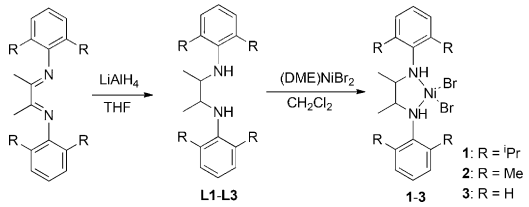

Scheme 1. Synthesis route of α-diamine nickel complexes.

of the reported ligands were fully characterized by ^{1}H NMR, ^{13}C NMR, ESI-MS, and elemental analysis. NMR analyses show that bulky ligand **L1** is a mixture of *meso* and *rac* diastereomers with a ratio of 1:2.4 whilst ligands **L2** and **L3** exist as a *rac* individual diastereomer (Supporting Information, Figures S1–S10). Two diastereomers of **L1** were readily separated by column chromatography on silica gel using *n*-hexane/dichloromethane (3:1) as the eluent, and were recrystallized from ethanol as white solids. The *rac* diastereomer of ligand **L1** was also found to be preferred 2:1 as determined by X-ray crystallographic analysis of the major product (Figure 2), while a single crystal of *rac*-**L2** was merely obtained (Figure 3).

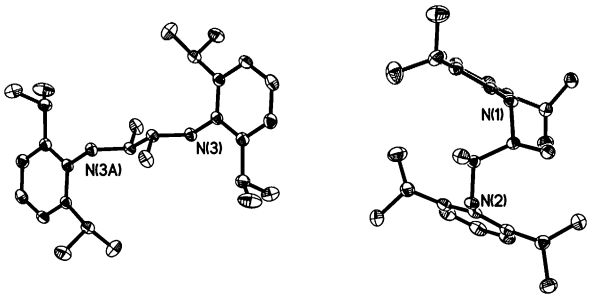

Figure 2. Molecular structure of ligand *meso*- and *rac*-**L1**. Hydrogen atoms are omitted for clarity; ellipsoids are set at 30% probability.

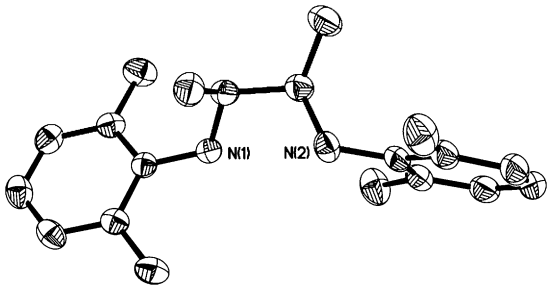

Figure 3. Molecular structure of ligand *rac*-**L2**. Hydrogen atoms are omitted for clarity; ellipsoids are set at 30% probability.

Nickel complexes **1**–**3** were obtained by addition of the ligands to a suspension of (DME)$NiBr_2$ in CH_2Cl_2 at room temperature (Scheme 1). Single crystals of nickel complexes **1** and **2** suitable for X-ray diffraction analysis were obtained by slow evaporation of the nickel complex solution in CH_2Cl_2. Complex **1** adopts a four-coordinate geometry for the nickel center (Figure 4), whilst the dimerization of complex **2** gives a five-coordinate geometry (Figure 5). Despite the same atom connec-

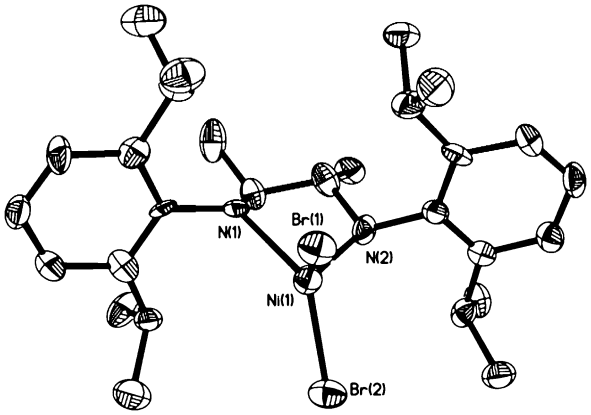

Figure 4. Crystal structure of α-diamine nickel complex **1**. Hydrogen atoms are omitted for clarity; ellipsoids are set at 30% probability.

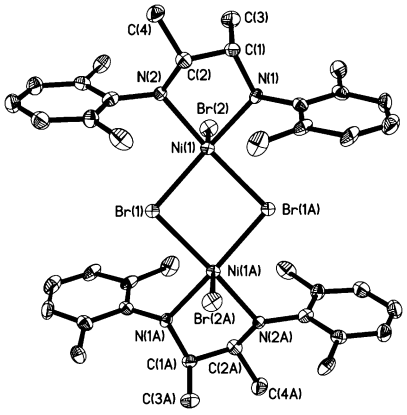

Figure 5. Crystal structure of α-diamine nickel complex **2**. Hydrogen atoms and two CH_2Cl_2 molecules are omitted for clarity; ellipsoids are set at 30% probability.

tivity, α-diamine nickel complex **1** showed different bond lengths to the α-diimine nickel analogue. The observed N–Ni (2.06 Å) and C–N (1.51 Å) bond lengths of α-diamine nickel **1** are longer than α-diimine nickel **4** ((ArN=C(Me)–(Me)C=NAr)-$NiBr_2$, Ar = 2,6-diisopropylphenyl; N–Ni 2.00 Å, C–N 1.28 Å).[10] The longer Ni–N distance presumably causes a reduction in the ethylene polymerization activity of the nickel catalyst by using α-diamine instead of α-diimine ligand.[9] Because the two sp^3 hybrid carbon atoms adopt tetrahedral configurations, the chelated ring (N-C-C-N-Ni) is significantly distorted. The two methyl groups on the backbone and the aniline moieties swing to two opposite sides, showing axially steric effects on the nickel metal. Besides, the bite angle of N-Ni-N of α-diamine nickel complex **1** is 82.07°, which is larger than those of amine–imine nickel (81.20°) and α-diimine nickel **4** (80.58°). This observation strongly suggests that there is an increased steric environment, including both axial and equatorial sites around the Ni metal, by changing the N–Ni combination from N(imine)–Ni to N(amine)–Ni. In contrast to the α-diimine nickel analogue, the α-diamine nickel complex **1** has a nonplanar chelate ring, twisted aniline moieties, and a large angle of N-Ni-N, which may cause distinctive steric effects on ethylene polymerization.

Ethylene polymerizations were carried out using nickel complexes **1**, **2**, and **3** activated by Et_2AlCl at various polymerization temperatures (Table 1). Steric effect of *o*-aryl substituents on polymerization activity and polymer molecular weight was firstly investigated. Polymerization results in Table 1 (entries 2, 3, 4 versus 9, 10, 11) show that reducing the steric hindrance of the α-diamine ligand by substituting the *o*-isopropyl groups with the *o*-methyl groups results in an increased polymerization activity. Catalyst **1** with isopropyl groups showed the highest activity of 25.9 kg PE (mol Ni)$^{-1}$ h^{-1} at 35 °C, whereas catalyst **2** with methyl groups exhibited about 7 times the activity at the optimized temperature of 0 °C (177.0 kg PE (mol Ni)$^{-1}$ h^{-1}). This steric effect of *o*-aryl substituents on ethylene polymerization activity conflicts with previous observations made using α-diimine nickel catalysts.[2d] Generally, α-diamine nickel catalysts are less active than α-diimine nickel catalysts and afford lower molecular weight PE,[2d,9c] partly because the α-diimine ligand is a stronger π-acceptor (planar chelate ring) than an α-diamine ligand (largely distorded chelate ring).[9g]

Table 1. Ethylene polymerization results using α-diamine nickel catalysts **1**–**3**/Et_2AlCl.[a]

Entry	Ni	*P* [psig]	*T* [°C]	Yield [g]	Act.[b]	M_n[c]	PDI[c]	Br[d]	T_m[e] [°C]	T_g[e] [°C]
1	**1**	3	−20	0.076	7.6	11.1	1.02	140	–[h]	−66
2	**1**	3	0	0.133	13.3	20.1	1.01	148	–	−66
3	**1**	3	20	0.207	20.7	29.9	1.02	139	–	−65
4	**1**	3	35	0.259	25.9	37.6	1.05	146	–	−67
5	**1**	3	50	0.200	20.0	24.8	1.29	137	–	−66
6	**1**	3	65	0.075	7.5	8.3	1.85	136	–	−69
7	**2**	3	−40	0.074	7.4	17.5	1.12	20	128	–
8	**2**	3	−20	0.623	62.3	128.2	1.13	44	102	–
9	**2**	3	0	1.770	177.0	218.7	1.07	105	−3	−56
10	**2**	3	20	0.373	37.3	76.1	1.63	137	–	−65
11	**2**	3	35	0.074	7.4	17.7	2.01	144	–	−68
12	**3**	3	−40	0.034	3.4	15.5	1.74	19	129	–
13	**3**	3	−20	0.122	12.2	11.5	1.94	39	107, 87	–
14	**3**	3	−10	0.228	22.8	5.6	1.61	87	−8	–
15	**3**	3	0	0.180	18.0	8.3	1.94	106	−31	–
16[f]	**1**	75	35	0.532	213	212.2	1.01	121	–	−63
17[f]	**1**	150	35	0.762	305	298.0	1.02	119	–	−60
18[g]	**2**	75	0	0.289	867	246.5	1.03	62	87	–
19[g]	**2**	150	0	0.493	1479	427.4	1.04	32	111	–

[a] Polymerization conditions: 10 mmol of nickel, Al/Ni = 200, 60 min, 29 mL toluene and 1 mL CH_2Cl_2. [b] Activity: kg PE (mol Ni)$^{-1}$ h^{-1}. [c] M_n [kg mol^{-1}] and PDI were determined by gel permeation chromatography (GPC) in 1,2,4-trichlorobenzene at 150 °C using a light-scattering detector. [d] Branching density; branches per 1000 carbon atoms determined by ^{1}H NMR spectroscopy. [e] Determined by DSC. [f] 5 mmol of nickel, 30 min, 59 mL toluene. [g] 2 mmol of nickel, 10 min, 59 mL toluene. [h] Not determined.

A different steric effect of the α-diamine nickel catalyst on polymer molecular weight is also observed, and a circa sixfold increase in polymer molecular weight can be observed by substitution of *o*-methyl groups for *o*-isopropyl groups. Generally, reducing steric hindrance can decrease the blocking of the axial position for α-diimine and amine–imine nickel catalysts with a planar chelate ring, thus leading to a drop in molecular weight because of the acceleration of chain transfer. Herein, both high catalyst activity and high polymer molecular weight can be successfully achieved by the α-diamine nickel catalyst **2** with *o*-methyl groups on the aryl substituents. This significant difference in steric effect is closely related to the steric environment around the nickel atom. Because the α-diamine nickel catalyst has a nonplanar chelate ring, the bulky isopropyl groups may block equatorial coordination sites, thus slowing down the trapping of ethylene. Higher molecular weight polymer obtained by the less bulky α-diamine nickel catalyst **2** can be attributed to a rapid ethylene insertion rate and axial steric effect of the two methyl groups on sp^3 carbon atoms (see the X-ray part of the Experimental Section) for suppressing chain transfer. A lack of the substitutents on N-aryl moiety decreases steric hindrance and leads to a remarkable drop in activity and molecular weight of the obtained polyethylene (PE), whereas molecular weight of the obtained PE is much higher than that of the PE produced by α-diimine nickel analogue (ArN = C(Me)-(Me)C=NAr)$NiBr_2$, Ar = phenyl (C4 and C6 oligomers).[11]

The polymerization results clearly demonstrate that steric effects influence the thermal stability of α-diamine nickel catalyst. Increasing steric hindrance of *o*-aryl substituents significantly enhances the thermal stability of the α-diamine nickel catalysts. Catalyst **1** is active in a wide range of temperatures from −20 to 65 °C, while catalyst **3** only displays apparent activity below 0 °C. Moreover, a huge drop of 96% activity is observed for catalyst **2** when the temperature is increased from 0 to 35 °C, whilst an increased activity is observed for catalyst **1**. This observation can be attributed to the protection and stabilization of the nickel metal center provided by bulky substituents. It is known that the classic α-diimine nickel catalyst **4** undergoes catalyst decomposition above 50 °C whereas α-diamine nickel catalyst **1** was found to maintain good catalytic activity at 50 °C although the coordinating ability of the imine is stronger than the amine group.[2d] A possible interpretation

is that C–H activation occurs by forming an equatorial co-plane between the nickel center and the isopropyl substituents because of N–C(aryl) rotations for α-diimine nickel catalyst, whereas, in case of α-diamine nickel catalyst **1** with two twisted aniline moieties, it hardly proceeds because of the abstraction of an equatorial co-plane.[2d, 3c,d, 8b]

It is noteworthy that narrowly dispersed polyethylene (PDI <1.1) can be formed using catalyst **1** below 35 °C or catalyst **2** below 0 °C, suggesting the reaction occurs in a living polymerization fashion. Figure 6 shows symmetric GPC traces of the polymers obtained at different polymerization times, which

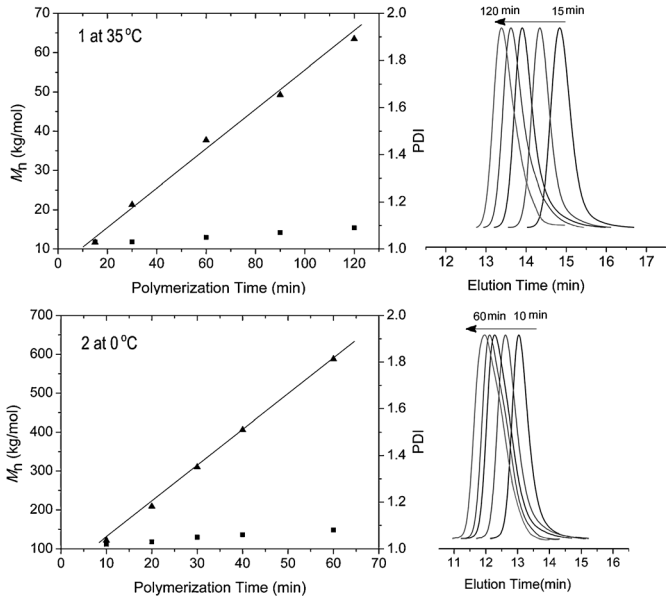

Figure 6. Plots of M_n (▲) and M_w/M_n (PDI) (■) as a function of polymerization time using **1**/Et_2AlCl at 35 °C (top) and **2**/Et_2AlCl at 0 °C (down). Polymerization conditions: 3 psig, 10 μmol **1**, and 2 μmol **2**, Al/Ni = 200). Right: GPC traces at different times using a light scattering detector.

shift to the higher molecular weight region with prolonged polymerization time. Plots of number-average molecular weights (M_n) as a function of polymerization time also illustrate that M_n grows linearly with the polymerization time, and M_w/M_n (PDI) values are below 1.10. Undoubtedly, the living polymerization of ethylene can be successfully achieved using **1**/Et_2AlCl at 35 °C or **2**/Et_2AlCl at 0 °C. MMAO compound can also replace Et_2AlCl as the activator for the living polymerization of ethylene using **1** at 35 °C, with polyethylene of a higher molecular weight being formed (Supporting Information, Table S9 and Figure S28). This kind of α-diamine nickel catalyst is one example of a rare late transition-metal catalytic system for the living polymerization of ethylene,[9a–d, 12] whereas α-diimine nickel catalyst **4** is known to polymerize ethylene in a nonliving fashion.[2d, 3a]

Chain walking is one of the most distinguishing features for nickel and palladium catalysts and is responsible for the generation of branched polyethylene.[1a,b] ^1H NMR analysis showed that the branching density of the obtained PE is closely related to the steric effect of *o*-aryl substituents. The same trend is observed in α-diimine nickel catalysts in that increasing steric hindrance leads to an increase in branching density, especially at low temperatures.[2d] Differently, steric effects of *o*-aryl substituents have a dramatic influence on dependence of branching density on polymerization conditions such as temperature and ethylene pressure. The branching density of PE obtained by catalyst **2** with methyl substituents increases with increased temperature and reduced ethylene pressure (Figure 7), which

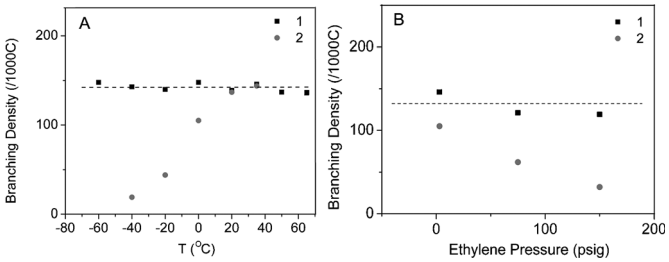

Figure 7. The dependency of branching density of PE obtained by **1** and **2**/Et_2AlCl on polymerization temperature and ethylene pressure.

is similar to previous observations regarding α-diimine nickel and amine–imine nickel catalysts.[2d, 9c] However, the bulky α-diamine catalyst **1** with isopropyl groups shows a similar observation to the α-diimine palladium catalyst in that the branching density of the PE is nearly independent to polymerization temperature and ethylene pressure (Figure 7). Even at very low polymerization temperatures (−40, −60 °C), the obtained PEs have high branching densities of about 140/1000C. Despite the mild change of total branching density within the tested ethylene pressure and temperature range for **1**/Et_2AlCl, the apparent morphology of the obtained PE changes from viscous oil at 3 psig to a white and elastic solid at 150 psig (Figure 8).

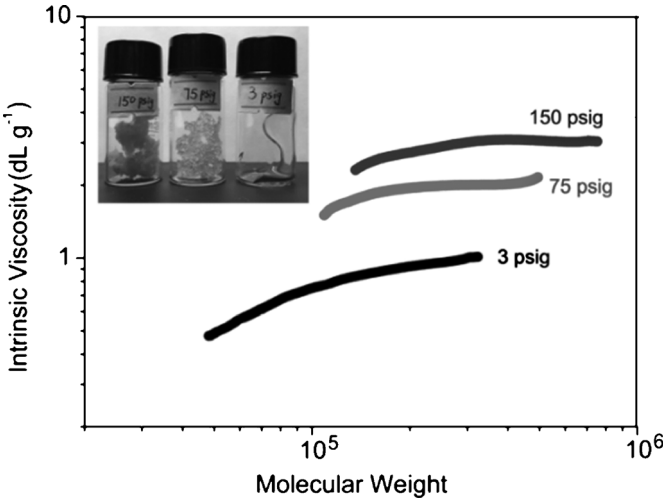

Figure 8. The dependency of intrinsic viscosity on molecular weight of the PEs obtained by **1**/Et_2AlCl at various ethylene pressures. Inset: Images of PE samples.

Branching distributions of the obtained PEs determined by ^{13}C NMR spectroscopy also revealed that the contents of long branches and the branch-on-branch structures generated through tertiary carbons (*sec*-butyl group; 19.44 and 11.72 ppm) increased gradually with reducing ethylene pressure and increasing temperature (Supporting Information, Table S6), suggesting a change of branching topology with variation in temperature and pressure.

Dilute solution properties also enable us to examine the branching topology of the PE obtained at different ethylene pressures. The dependency of intrinsic viscosity on polymer molecular weight detected by high-temperature gel permeation chromatography with a viscosity detector can directly reflect the branching topology of the PE. As shown in Figure 8, the intrinsic viscosity of the obtained PE increases with increasing polymerization pressure under the same molecular weight. These results strongly indicate that the PE topology changes, and linear PE with moderate branching is formed at a high pressure of 150 psig, whereas hyperbranched PE (HBPE) is produced at a low pressure of 3 psig using the **1**/Et_2AlCl system. Generally, the bulky nickel catalyst **1** showed a different chain-walking feature to the reported nickel catalyst in that it can tune the branching topology while maintaining the same level of branching density. In contrast to previous work on controlling the branching topology of PE by noble α-diimine palladium catalysts, the nickel-based catalyst **1** is cheaper, and the difficulty in separation and purification of hyperbranched PE is significantly decreased because palladium black formation can be avoided.[6,7]

Considering the fact that the polymerization activity of catalyst **1** is nearly insensitive to ethylene pressure but that of catalyst **2** is significantly sensitive, a general mechanism for ethylene polymerization with α-diamine nickel catalysts is proposed in combination with chain walking for branch formation (Scheme 2).[13] Cationic nickel species for ethylene polymerization are generated by the activation of nickel dihalide complexes with alkylaluminum compounds. On the basis of single-crystal X-ray diffraction analysis, α-diamine nickel catalysts adopt a distorted ring system because of the two sp^3 hybrid nitrogen donor atoms. The resting state of bulky catalyst **1** is solely an alkyl olefin species **A** because bulky isopropyl groups may suppress the formation of the β-agostic complex (**B**). Therefore, branching density is independent to ethylene pressure and temperature, which is similar to the α-diimine palladium catalyst.[14] The resting state of the less bulky catalyst **2** can predominantly be the β-agostic complex (**B**), and branching density thereby decreases with increasing pressure and reducing temperature.[14] Various branches originate from the chain-walking process involving β-hydride elimination and reinsertion. Branching density and topology is a result of the competition between ethylene insertion and chain walking. For catalyst **1**, the trapping of ethylene is slow and the catalyst may walk multiple carbons before being trapped, leading to the formation of a hyperbranched topology, especially at low ethylene pressure. The ethylene polymerization results using **1**/Et_2AlCl over the range of Al/Ni ratio from 100 to 800 (Supporting Information, Table S10) show that there is no substantial change in catalytic activity, molecular weight, and polydispersity of the obtained polymers, strongly indicating no occurrence of chain transfer to the aluminum co-catalyst. Therefore, chain-transfer reactions should occur though associative displacement or chain transfer to bound monomer at high temperatures.[1,2]

Conclusions

In summary, we have successfully developed conveniently accessible novel α-diamine nickel catalysts. Reducing the steric hindrance of the α-diamine ligand by substituting the *o*-isopropyl groups with the *o*-methyl groups results in increased polymerization activity and molecular weight at the cost of thermal stability. Living polymerization of ethylene can be achieved using α-diamine nickel catalysts **1** or **2** by the suppression of chain-transfer reactions. The bulky α-diamine nickel catalyst **1** with isopropyl substituents can also control the branching topology of PE at the same level of branching density by tuning reaction temperature and ethylene pressure. This kind of α-diamine nickel catalyst is a promising candidate for a deep and fundamental understanding of late transition-metal-catalyzed olefin polymerizations from a coordination geometry point of view. Further optimization of α-diamine framework and the α-olefin polymerization reactions are ongoing.

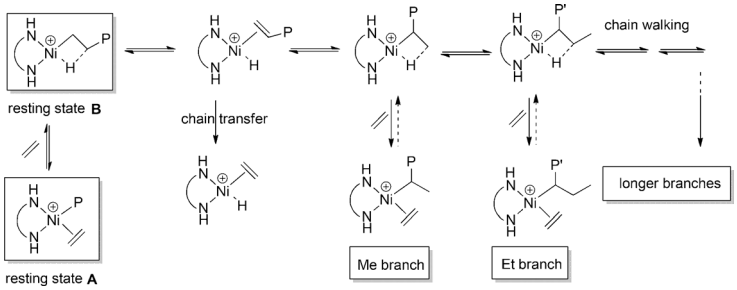

Scheme 2. Proposed mechanism for α-diamine nickel-catalyzed ethylene polymerization.

Experimental Section

All manipulations involving air- and moisture sensitive compounds were carried out under an atmosphere of dried and purified nitrogen using standard vacuum-line, Schlenk, or glovebox techniques. Dichloromethane was dried over phosphorus pentoxide for 8 h, and distilled under nitrogen atmosphere. Toluene, hexane, and tetrahydrofuran (THF) were refluxed over from Na/K alloy. Butane-2,3-dione, aniline, 2,6-dimethylaniline, 2,6-diisopropylaniline, and $(DME)NiBr_2$ were purchased from Aldrich and used as received. MMAO (7 wt% Al in heptane) was purchased from Akzo-Nobel and used as received. Diethylaluminium chloride (Et_2AlCl, 1.0 M in hexane) and lithium aluminum hydride ($LiAlH_4$, 95%, powder) were purchased from Acros. Ethylene (99.99%) was purified by passing through Agilent moisture and

oxygen traps. Other commercially available reagents were purchased and used without purification.

Measurements

Elemental analyses were performed on a Vario EL microanalyzer. Mass spectra were obtained using electrospray ionization (ESI) LCMS-2010 A (for ligands) or fast atom bombardment (FAB) LCQ DECA XP (for nickel complexes). NMR spectra of organic compounds were carried out on a Bruker 400 MHz instrument in $CDCl_3$ using TMS as a reference. ^{13}C NMR spectra of polymers were carried out on a Bruker 500 MHz at 120 °C. Sample solutions of the polymer were prepared in *o*-$C_6H_4Cl_2$/*o*-$C_6D_4Cl_2$ (50% v/v) in a 10 mm sample tube. The spectra of the quantitative ^{13}C NMR were taken with a 74° flip angle, an acquisition time of 1.5 s, and a delay of 4.0 s. The chemical shifts were referenced to main chain of PE ($-(CH_2)_n-$) (30 ppm). DSC analyses were conducted with a PerkinElmer DSC-7 system. The DSC curves were recorded as second heating curves from −100 to 140 °C at a heating rate of 10 °C min^{-1} and a cooling rate of 10 °C min^{-1}. GPC analysis of the molecular weights and molecular weight distributions (PDI = M_w/M_n) of the polymers at 150 °C were performed on a PL-GPC 220 high-temperature chromatograph equipped with a triple-detection array, including a differential refractive-index detector, a two-angle light-scattering detector, and a four-bridge capillary viscometer. The detection angles of the LS detector were 15 and 90°, and the laser wavelength was 658 nm. 1,2,4-Trichlorobenzene (TCB) was used as the eluent at a flow rate of 1.0 mL min^{-1}.

Crystal structure determination

The crystals were mounted on a glass fiber and transferred to a Bruker CCD platform diffractometer. Data obtained with the ω-2θ scan mode was collected on a Bruker SMART 1000 CCD diffractometer with graphite-monochromated Cu or Mo. The structures were solved using direct methods, while further refinement with full-matrix least square on F^2 was obtained with the SHELXTL program package. All non-hydrogen atoms were refined anisotropically. Hydrogen atoms were introduced in calculated positions with the displacement factors of the host carbon atoms. Crystal data and structural refinement for the four structures are collated in Table S1. CCDC 1453215 (**1**), 1453216 (**2**), 1453217 (**L1**), and 1453218 (**L2**) contain the supplementary crystallographic data for this paper. These data can be obtained free of charge from The Cambridge Crystallographic Data Centre.

Atmospheric-pressure ethylene polymerization

A round-bottom Schlenk flask with stirring bar was heated for 3 h at 150 °C under vacuum and then cooled to room temperature. The flask was pressurized to 15 psig of ethylene and vented three times. The appropriate alkyl aluminum compound as co-catalyst and toluene were added into the glass reactor under 3 psig of ethylene. The system was continuously stirred for 5 min, and then toluene and 1 mL of a solution of nickel complex in CH_2Cl_2 were added sequentially by syringe to the well-stirred solution, and the total reaction volume was kept at 30 mL. The ethylene pressure was kept constant at 3 psig by the continuous feeding of gaseous ethylene throughout the reaction. The other reaction temperatures were controlled with an external oil bath or a cooler in polymerization experiments. The polymerizations were terminated by the addition of 200 mL of acidic methanol (95:5 ethanol/HCl) after continuously stirring for an appropriate period. The resulting precipitated polymers were collected and treated by filtration, washed with methanol several times, and dried under vacuum at 40 °C to a constant weight.

High-pressure polymerization of ethylene

A mechanically stirred 100 mL Parr reactor was heated to 150 °C for 2 h under vacuum and then cooled to room temperature. The autoclave was pressurized to 100 psig of ethylene and vented three times. The autoclave was then charged with solution of Et_2AlCl in toluene under 3 psig of ethylene at initialization temperature. The system was maintained by continuously stirring for 5 min, and then a 1 mL solution of the nickel complex in CH_2Cl_2 was charged into the autoclave under 3 psig of ethylene. The ethylene pressure was raised to the specified value. The reaction temperature was controlled by means of a water bath and found to be ±2 °C as monitored by an internal thermocouple. The reaction was carried out for a certain time. Polymerization was terminated by addition of acidic methanol after releasing ethylene pressure. The resulting precipitated polymers were collected and treated by filtration, washed with methanol several times, and dried under vacuum at 40 °C to a constant weight.

Synthesis of α-diimine compounds

α-Diimine compounds were prepared according to the reported procedure. A solution of substituted anilines (2 equiv) in ethanol in the presence of formic acid was added to a solution of butane-2,3-dione (1.72 g, 20 mmol) in ethanol (50 mL). The solution was allowed to stir for 5 h at 50 °C, and cooled to −20 °C overnight. The yellow crystalline solids were collected by filtration and washed with cold ethanol to provide the isolated product in good yield.

Synthesis of α-diamine ligands

Ar–NH–C(Me)–(Me)C–NH–Ar (Ar = 2,6-diisopropylphenyl) (L1): A solution of α-diimine compound (Ar–N=C(Me)–(Me)C=N–Ar (Ar = 2,6-diisopropylphenyl)) (0.81 g, 2 mmol) in THF (30 mL) was slowly added to a suspension of $LiAlH_4$ (0.31 g, 8.2 mmol) in THF (40 mL) under a nitrogen atmosphere over a period of 5 min at 0 °C. The mixture was then heated to 50 °C overnight. After cooling to 0 °C using ice/water bath, the reaction mixture was carefully hydrolyzed with a 10% aqueous NaOH solution. The organic layer was separated and washed with water three times, and dried over $MgSO_4$. The solvent was then evaporated off, and the resulting pale yellow oil was dissolved in hot ethanol and the solution cooled to room temperature to give a white solid. Yield: 0.72 g, 88%. Diastereomers were separated by column chromatography on silica gel using *n*-hexane/dichloromethane (75:25) as the eluent, and were recrystallized from ethanol as white solids with a ratio of 2.4:1 determined by ^1H NMR spectroscopy. ^1H NMR ($CDCl_3$, 400 MHz): *meso*-diastereomer: δ = 7.10 (d, 4H, Ar-*H*), 7.03 (t, 2H, Ar-*H*), 3.60 (s, 2H, N*H*), 3.52–3.45 (m, 2H, C*H*(CH_3)), 3.40 (sep, 4H, C*H*(CH_3)$_2$), 1.22 (dd, 24H, C*H*(CH_3)$_2$), 1.01 ppm (d, 6H, CH(C*H*$_3$)); *rac*-diastereomer: 7.10–6.99 (m, 6H, Ar-*H*), 3.37–3.17 (m, 8H, N*H* + C*H*(CH_3)$_2$ + NC*H* (CH)(CH_3)), 1.19 (dd, 24H, C*H*(CH_3)$_2$), 1.11 ppm (dd, 6H, CH(C*H*$_3$)); ^{13}C NMR (100 MHz, $CDCl_3$): *rac*-diastereomer: δ = 142.63, 141.35, 123.48, 123.35, 59.66, 27.78, 24.35, 23.92, 15.68 ppm; *meso*-diastereomer: 141.80, 141.64, 123.49, 122.73, 58.86, 27.72, 24.18, 23.91, 15.50 ppm; ESI-MS (*m/z*): 411, 410, 409 [M^++1]; elemental analysis calcd for $C_{28}H_{44}N_2$: C 82.99, H 10.85, N 6.85; found: C 82.75, H 11.10, N 6.88.

Ar–NH–C(Me)–(Me)C–NH–Ar (Ar = 2,6-dimethylphenyl) (L2): Following the above procedure, ligand **L2** Ar–NH–C(Me)–(Me)C–NH–Ar (Ar = 2,6-dimethylphenyl) was isolated as white solid in

91% yield. ^{1}H NMR ($CDCl_3$, 400 MHz): δ = 6.99 (d, 4H, Ar-*H*), 6.80 (t, 2H, Ar-*H*), 3.63 (s, 4H, N*H*, *CH*CH_3), 2.30 (s, 12H, *CH*$_3$), 1.02 ppm (d, 6H, CH*CH*$_3$). ^{13}C NMR (100 MHz, $CDCl_3$): δ = 144.61, 129.06, 129.01, 121.22, 55.51, 19.40, 16.10 ppm; ESI-MS (*m/z*): 299, 298, 297 [M^++1]; elemental analysis calcd for $C_{20}H_{28}N_2$: C 81.03, H 9.52, N 9.45; found: C 81.23, H 9.56, N 9.53.

Ar–NH–C(Me)–(Me)C–NH–Ar (Ar = phenyl) (L3): Following the above procedure, ligand **L3** Ar–N–C(Me)–(Me)C–N–Ar (Ar = phenyl) was isolated as colorless oil in 93% yield. ^{1}H NMR ($CDCl_3$, 400 MHz): δ = 7.20(m, 4H, Ar-*H*), 6.73 (m, 6H, Ar-*H*), 3.74 (s, 2H, N*H*), 3.63 (m, 2H, -*CH*-CH_3), 1.22 ppm (d, 6H, *CH*$_3$); ^{13}C NMR (100 MHz, $CDCl_3$): δ = 147.7, 129.5, 129.4, 117.7, 117.6, 113.8, 113.6, 52.6, 52.3, 17.1, 16.35 ppm; elemental analysis calcd for $C_{16}H_{20}N_2$: C 79.96, H 8.39, N 11.66; found: C 79.92, H 8.37, N 11.63; ESI-MS (*m/z*): 243, 242, 241 [M^++1].

Synthesis of α-diamine nickel complexes

[Ar–NH–C(Me)–(Me)C–NH–Ar]NiBr$_2$ (Ar = 2,6-diisopropylphenyl) (1): A solution of ligand **L1** (420 mg, 1.03 mmol) in 10 mL dichloromethane was added to a stirred suspension of (DME)$NiBr_2$ (DME = 1,2-dimethoxyethane; 308 mg, 1.00 mmol) in dichloromethane (30 mL) under a nitrogen atmosphere at room temperature. After the addition of the ligand, the solution began to turn dark red. After stirring for 6 h, the solution was filtered through celite, and the solvent of the filtrate was removed in vacuum. The residue was recrystallized from dichloromethane–hexane to give a purple-red powder in 63% yield (393 mg). Single crystals were grown from a dichloromethane solution at room temperature in glovebox. FAB-MS (*m/z*): 548, 547, 546 [M–Br]$^+$; 468, 467, 466 [M–2Br]$^+$; 410, 409 [ligand]$^+$; elemental analysis calcd for $C_{28}H_{44}Br_2N_2Ni$: C 53.62, H 7.07, N 4.47; found: C 53.49, H 7.01, N 4.42.

[Ar–NH–C(Me)–(Me)C–NH–Ar]NiBr$_2$(Ar = 2,6-dimethylphenyl) (2): Following the above procedure, the reaction of (DME)$NiBr_2$ (308 mg, 1.00 mmol) and ligand **L2** (305 mg, 1.03 mmol) gave a yellow powder in 65% yield (333 mg). Single crystals were grown from a dichloromethane solution at room temperature in a glovebox. FAB-MS (*m/z*): 435, 434, 433 [M–Br]$^+$; 355, 354, 353 [M–2Br]$^+$; 297, 296, 295 [ligand]$^+$; elemental analysis calcd for $C_{20}H_{28}Br_2N_2Ni$: C 46.65, H 5.48, N 5.44; found: C 46.51, H 5.41, N 5.38.

[Ar–NH–C(Me)–(Me)C–NH–Ar]NiBr$_2$ (Ar = phenyl) (3): Following the above procedure, the reaction of (DME)$NiBr_2$ (308 mg, 1.00 mmol) and ligand Ar–N–C(Me)–(Me)C–N–Ar (Ar = phenyl; 250 mg, 1.04 mmol) gave a red powder in 69% yield (312 mg). FAB-MS (*m/z*): 379, 378, 376 [M–Br]$^+$; 300, 299, 298[M–2Br]$^+$; 242, 241[ligand]$^+$; elemental analysis calcd for $C_{16}H_{20}Br_2N_2Ni$: C 41.88, H 4.39, N 6.11; found: C 41.83, H 4.36, N 6.08.

Acknowledgements

This work was supported by grants from the National Natural Science Foundation of China (NSFC; Projects 21374134 and 21274167), Natural Science Foundation of Guangdong Province (1414050000552), Science and Technology Planning Project of Guangdong Province (201510010070), Technology Innovation Project of Educational Commission of Guangdong Province of China (2013KJCX0002), the Fundamental Research Funds for the Central Universities (15lgzd03), and CNPC Innovation Foundation (2014D-5006-0502).

Keywords: branching topology · homogeneous catalysis · living polymerization · N ligands · nickel

[1] a) L. K. Johnson, C. M. Killian, M. Brookhart, *J. Am. Chem. Soc.* **1995**, *117*, 6414–6415; b) L. K. Johnson, S. Mecking, M. Brookhart, *J. Am. Chem. Soc.* **1996**, *118*, 267–268; c) S. D. Ittel, L. K. Johnson, M. Brookhart, *Chem. Rev.* **2000**, *100*, 1169–1203; d) S. Mecking, *Angew. Chem. Int. Ed.* **2001**, *40*, 534–540; *Angew. Chem.* **2001**, *113*, 550–557; e) G. W. Coates, P. D. Hustad, S. Reinartz, *Angew. Chem. Int. Ed.* **2002**, *41*, 2236–2257; *Angew. Chem.* **2002**, *114*, 2340–2361; f) E. Y. X. Chen, T. J. Marks, *Chem. Rev.* **2000**, *100*, 1391–1434; g) T. M. J. Anselment, S. I. Vagin, B. Rieger, *Dalton Trans.* **2008**, 4537–4548; h) J. D. Azoulay, R. S. Rojas, A. V. Serrano, H. Ohtaki, G. B. Galland, G. C. Bazan, *Angew. Chem. Int. Ed.* **2009**, *48*, 1089–1092; *Angew. Chem.* **2009**, *121*, 1109–1112; i) C. Chen, S. Luo, R. F. Jordan, *J. Am. Chem. Soc.* **2010**, *132*, 5273–5284.

[2] a) D. H. Camachoa, Z. Guan, *Chem. Commun.* **2010**, *46*, 7879–7893; b) S. Mecking, L. K. Johnson, L. Wang, M. Brookhart, *J. Am. Chem. Soc.* **1998**, *120*, 888–899; c) S. A. Svejda, L. K. Johnson, M. Brookhart, *J. Am. Chem. Soc.* **1999**, *121*, 10634–10635; d) D. P. Gates, S. A. Svejda, E. Onate, C. M. Killian, L. K. Johnson, P. S. White, M. Brookhart, *Macromolecules* **2000**, *33*, 2320–2334.

[3] a) F. Liu, H. Hu, Y. Xu, L. Guo, S. Zai, K. Song, H. Gao, L. Zhang, F. Zhu, Q. Wu, *Macromolecules* **2009**, *42*, 7789–7796; b) L. Guo, H. Gao, Q. Guan, H. Hu, J. Deng, J. Liu, F. Liu, Q. Wu, *Organometallics* **2012**, *31*, 6054–6062; c) J. L. Rhinehart, L. A. Brown, B. K. Long, *J. Am. Chem. Soc.* **2013**, *135*, 16316–16319; d) J. L. Rhinehart, N. E. Mitchell, B. K. Long, *ACS Catal.* **2014**, *4*, 2501–2504; e) S. Dai, X. Sui, C. Chen, *Angew. Chem. Int. Ed.* **2015**, *54*, 9948–9953; *Angew. Chem.* **2015**, *127*, 10086–10091; f) L. Guo, S. Dai, X. Sui, C. Chen, *ACS Catal.* **2016**, *6*, 428–441.

[4] a) N. A. Eckert, E. M. Bones, R. J. Lachicotte, P. L. Holland, *Inorg. Chem.* **2003**, *42*, 1720–1725; b) J. Zhang, H. Gao, Z. Ke, F. Bao, F. Zhu, Q. Wu, *J. Mol. Catal. A* **2005**, *231*, 27–34.

[5] a) H. Gao, W. Guo, F. Bao, G. Gui, J. Zhang, F. Zhu, Q. Wu, *Organometallics* **2004**, *23*, 6273–6280; b) H. Gao, J. Zhang, Y. Chen, F. Zhu, Q. Wu, *J. Mol. Catal. A* **2005**, *240*, 178–185; c) H. Gao, Y. Chen, F. Zhu, Q. Wu, *J. Polym. Sci. Part A* **2006**, *44*, 5237–5246; d) H. Gao, Z. Ke, L. Pei, K. Song, Q. Wu, *Polymer* **2007**, *48*, 7249–7254; e) H. Gao, L. Pei, K. Song, Q. Wu, *Eur. Polym. J.* **2007**, *43*, 908–914.

[6] a) T. R. Younkin, E. F. Connor, J. I. Henderson, S. K. Friedrich, R. H. Grubbs, D. A. Bansleben, *Sciences* **2000**, *287*, 460–462; b) C. Wang, S. Friedrish, T. R. Younkin, R. H. Grubbs, *Organometallics* **1998**, *17*, 3149–3151.

[7] a) B. L. Small, M. Brookhart, A. M. A. Bennett, *J. Am. Chem. Soc.* **1998**, *120*, 4049–4050; b) G. J. P. Britovsek, V. C. Gibson, B. S. Kimberley, P. J. Maddox, S. J. McTavish, G. A. Solan, A. J. P. White, D. J. Williams, *Chem. Commun.* **1998**, 849–850; c) G. J. P. Britovsek, M. Bruce, V. C. Gibson, B. S. Kimberley, P. J. Maddox, S. Mastroianni, S. J. McTavish, C. Redshaw, G. A. Solan, S. Stromberg, A. J. P. White, D. J. Williams, *J. Am. Chem. Soc.* **1999**, *121*, 8728–8740; d) L. Guo, H. Gao, L. Zhang, F. Zhu, Q. Wu, *Organometallics* **2010**, *29*, 2118–2125; e) Z. Flisak, W. Sun, *ACS Catal.* **2015**, *5*, 4713–4724.

[8] a) D. Meinhard, M. Wegner, G. Kipiani, A. Hearley, P. Reuter, S. Fischer, O. Marti, B. Rieger, *J. Am. Chem. Soc.* **2007**, *129*, 9182–9191; b) D. H. Camacho, E. V. Salo, J. W. Ziller, Z. Guan, *Angew. Chem. Int. Ed.* **2004**, *43*, 1821–1825; *Angew. Chem.* **2004**, *116*, 1857–1861; c) D. H. Camacho, Z. Guan, *Macromolecules* **2005**, *38*, 2544–2546; d) H. Zou, F. M. Zhu, Q. Wu, J. Y. Ai, S. A. Lin, *J. Polym. Sci. Part A* **2005**, *43*, 1325–1330.

[9] a) S. Zai, F. Liu, H. Gao, C. Li, G. Zhou, L. Guo, L. Zhang, F. Zhu, Q. Wu, *Chem. Commun.* **2010**, *46*, 4321–4323; b) S. Zai, H. Gao, Z. Huang, H. Hu, H. Wu, Q. Wu, *ACS Catal.* **2012**, *2*, 433–440; c) H. Gao, H. Hu, F. Zhu, Q. Wu, *Chem. Commun.* **2012**, *48*, 3312–3314; d) H. Hu, L. Zhang, H. Gao, F. Zhu, Q. Wu, *Chem. Eur. J.* **2014**, *20*, 3225–3233; e) H. Gao, Y. Liu, G. Li, Z. Xiao, G. Liang, Q. Wu, *Polym. Chem.* **2014**, *5*, 6012–6018; f) H. Hu, H. Gao, D. Chen, G. Li, Y. Tan, G. Liang, F. Zhu, Q. Wu, *ACS Catal.* **2015**, *5*, 122–128; g) H. Hu, D. Chen, H. Gao, L. Zhong, Q. Wu, *Polym. Chem.* **2016**, *7*, 529–537.

[10] S. B. Clara, P. T. Gomes, M. Gomes, T. Duarte, *J. Organomet. Chem.* **2014**, *760*, 101–107.

[11] C. M. Killian, L. K. Johnson, M. Brookhart, *Organometallics* **1997**, *16*, 2005–2007.

[12] a) A. C. Gottfried, M. Brookhart, *Macromolecules* **2001**, *34*, 1140 – 1142; b) A. C. Gottfried, M. Brookhart, *Macromolecules* **2003**, *36*, 3085 – 3100; c) K. Zhang, Z. Ye, R. Subramanian, *Macromolecules* **2008**, *41*, 640 – 649; d) Y. Zhang, Z. Ye, *Chem. Commun.* **2008**, 1178 – 1180; e) J. D. Azoulay, Y. Schneider, G. B. Galland, G. C. Bazan, *Chem. Commun.* **2009**, 6177 – 6179.

[13] W. Sun, *Adv. Polym. Sci.* **2013**, *258*, 163 – 178.

[14] a) D. J. Tempel, L. K. Johnson, R. L. Huff, P. S. White, M. Brookhart, *J. Am. Chem. Soc.* **2000**, *122*, 6686 – 6700; b) D. Zhang, E. T. Nadres, M. Brookhart, O. Daugulis, *Organometallics* **2013**, *32*, 5136 – 5143.

Received: May 24, 2016
Revised: July 12, 2016
Published online on ■■ ■■, 0000

FULL PAPER

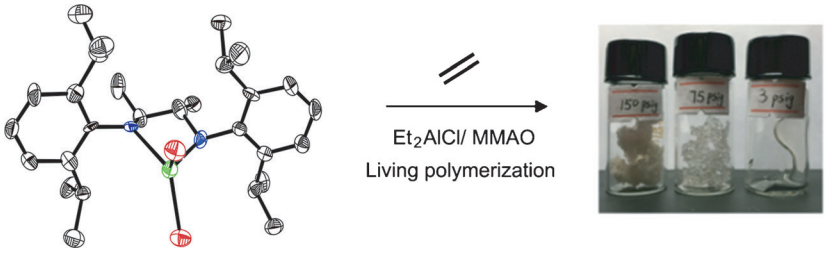

Novel α-diamine nickel complexes (see picture; Ni green, N blue, Br red) with nonplanar chelate rings catalyze ethylene polymerization in a living fashion. The bulky catalyst with isopropyl substituents can be used to control the branching topology of polyethylene upon tuning the reaction temperature and ethylene pressure.

Homogeneous Catalysis

H. Liao, L. Zhong, Z. Xiao, T. Zheng, H. Gao, Q. Wu*

■■ – ■■

α-Diamine Nickel Catalysts with Nonplanar Chelate Rings for Ethylene Polymerization